ACS Catalysis

Research Article

pubs.acs.org/acscatalysis

Surface Ti^{3+}-Containing (blue) Titania: A Unique Photocatalyst with High Activity and Selectivity in Visible Light-Stimulated Selective Oxidation

Mohamed S. Hamdy,[†,‡] Rezvaneh Amrollahi,[†,§] and Guido Mul*[,†]

[†]Photocatalytic Synthesis Group, Faculty of Science and Technology, MESA+ Institute for Nanotechnology, University of Twente, Enschede, The Netherlands

[‡]Chemistry Department, Faculty of Science, Helwan University, Cairo, Egypt

[§]Iran University of Science and Technology, Tehran, Iran

Supporting Information

ABSTRACT: A one-step synthesis procedure at elevated temperature was used to prepare Ti^{3+}-containing blue titania. The prepared material was characterized by X-ray powder diffraction (XRD), UV−vis, Raman, and X-ray photoelectron spectroscopy (XPS), and N_2 adsorption and desorption measurements. The blue titania sample was found to be crystalline, with a surface area of 22 m^2/g. Its phase composition consists of 85% rutile and 15% anatase with a multitude of defect surface V_O-Ti^{3+} sites. The blue titania showed an absorption red-shifted as compared to that of rutile, with a calculated bandgap of 2.93 eV. The photocatalytic performance of the blue titania was evaluated in the liquid phase selective photo-oxidation of methylcyclohexane (MCH) by illumination at 375 ± 10 nm (UV) and 425 ± 10 nm (visible light). The activity was monitored by attenuated total reflectance−Fourier transform infrared analysis. A high activity was observed for blue TiO_2, remarkably equal in magnitude at both investigated wavelengths. The activity of the blue titania surpassed the activity of other (commercial) titania catalysts (rutile and P25), in particular at 425 nm, and the obtained selectivity for ketones was also greater. The activity data are discussed in relation to the properties of the three catalysts investigated, i.e., the texture, phase composition, and presence or absence of surface defects, of which the latter appears to be dominant in explaining the performance of the blue titania.

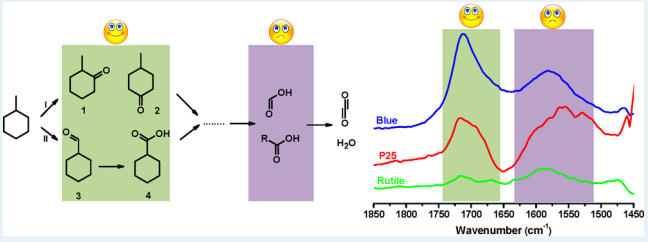

KEYWORDS: *self-doped TiO_2, blue titania, Ti^{3+}, photocatalysis, selective photo-oxidation, ATR, infrared, methylcyclohexane*

INTRODUCTION

Titanium dioxide (TiO_2) has been studied extensively in the field of photocatalysis. It attracts interest because of its nontoxicity, low cost, chemical inertness, and availability. It has a great ability to decompose undesired compounds present in air and water and is of interest for splitting water into oxygen and hydrogen. Finally, photoactivated titanium dioxide holds promise in selective chemical conversions. Unfortunately, because of its wide bandgap (i.e., 3.05 eV for rutile and 3.2 eV for anatase), TiO_2 exhibits high activity only under ultraviolet (UV) exposure, which limits its applicability in practice. More effective use of light emission of mercury lamps, commercially applied in large scale reactors, will make the application of photocatalysis to produce industrially relevant compounds or intermediates economically more attractive.

Several studies have been reported to shift the absorption of TiO_2 toward the visible light region such as doping titana with metal (e.g., V,[1] Cr,[2] Fe,[3] etc.) or nonmetal ions (e.g., N),[4] or by dye sensitization.[5] Also, reduction of the TiO_2 composition can lead to visible light absorption. Recently, reduced titania (TiO_{2-x}), which contains oxygen vacancies, V_O-Ti^{3+}, has been reported to exhibit significant photocatalytic activity in the visible light region in the water decomposition reaction.[6] Furthermore, a novel one-step synthesis of self-doped Ti^{3+} was reported.[7] The prepared blue material was again found to be effective in water splitting upon activation by visible light, when equipped with a cocatalyst (Pt). Besides changing the optical properties, earlier work of Liu et al.[8] demonstrated that the activity of surfaces containing Ti^{3+} prepared by hydrogen treatment differs markedly from that of stoichiometric TiO_2 surfaces in decomposition of water contaminants (sulfosalicylic acid and phenol) when excited by UV wavelengths. It has also been discussed[9] that surface defects associated with Ti^{3+} grow with an increase in crystallite size and enhance the activity in photocatalytic combustion of ethylene in air. Several techniques were reported to produce reduced TiO_2 containing surface Ti^{3+} for fundamental material science studies, such as thermal treatment under vacuum,[10] thermal annealing to high temperatures of >500 K,[11] thermal treatment with reducing conditions,

Received: September 10, 2012
Revised: October 8, 2012
Published: October 18, 2012

e.g., C^{12} and H_2,[8] laser treatment,[13] or high-energy particle (e.g., neutron or γ-ray)[14,15] bombardment.

Here we report for the first time the use of an unpromoted, surface Ti^{3+}-containing TiO_2 composition in the conversion of methylcyclohexane (MCH) to form methylcyclohexanone, as a model reaction for many interesting conversions in synthetic chemistry. Methylcyclohexane has a relatively low vapor pressure, which simplifies spectroscopic analysis of the reaction. Furthermore, methylcyclohexanone is used (i) as a solvent in making lacquers, varnishes, and plastics, (ii) in the leather industry, and (iii) as a rust remover. The photocatalytic study was conducted under UV (375 nm) or visible light (425 nm) illumination. Remarkably, the activity and selectivity were very similar at both wavelengths and significantly higher than those of commercial rutile and P25. We have characterized the prepared sample by several techniques in detail. We conclude that surface Ti^{3+} sites provide the unique activity and selectivity in the target reactions at relatively high wavelengths, and that the phase composition has a minor effect.

EXPERIMENTAL SECTION

Methylcyclohexene (MCH) and rutile (nanopowder, 99.5%) were obtained from Sigma-Aldrich, and P25 was obtained from Evonik. MCH, rutile, and P25 were used as received without any further modification. Reduced (blue) titania was prepared as reported by Feng et al.[7] A solution of 10 g of ethanol (99.5%, Sigma Aldrich), 2.5 g of hydrochloric acid (37%, Aldrich), 2 g of titanium(IV) isopropoxide (98%, Sigma), and 1.8 g of 2-ethylimidazole (98%, Sigma) was stirred for a period of 15 min at 350 rpm and subsequently introduced with caution into a preheated oven, located inside a fumehood, at 773 K in a porcelain crucible. The oven was closed during the duration of the synthesis. The evaporation and combustion of the solution in air for a period of 5 h produced a bluish, greyish powder.

The crystal structure of the material was determined in air by powder X-ray diffraction (XRD) using a Philips PW2050 (X'Pert-APD) diffractometer with Cu Kα radiation (λ = 0.15406 nm). Data were collected varying 2θ between 20° and 80° with a step size of 0.005° and a step time of 1 s. The anatase:rutile ratio was estimated from the following equation:

$$X_R = 1.26I_R/(I_A + 1.26I_R)$$

where X_R is the rutile fraction and I_R and I_A are the strongest intensities of the rutile (110) and anatase (101) diffraction pattern, respectively. Nitrogen physisorption measurements were taken at 77 K with a Micromeritics Tristar system (ASAP 2400) to determine the textural properties. Prior to the adsorption measurements, the samples were degassed at 573 K and 10^{-3} Pa for 24 h. The specific surface areas were calculated according to the Brunauer–Emmet–Teller (BET) method. Raman spectra were recorded with a Bruker Senterra Raman Spectrometer equipped with a N_2-cooled CCD detector (213 K). A green (λ = 532 nm) laser with an intensity of 2 mW was used for excitation. Spectra were acquired at a resolution of 9–15 cm^{-1}, and 10 scans were accumulated for each spectrum. X-ray photoelectron spectroscopy (XPS) was conducted using a Quantera SXM spectrometer made by Physical Electronics. The radiation was provided by a monochromatized Al Kα (1486.6 eV) X-ray source, operated at a 25 W emission power and a 15 kV acceleration voltage. Diffuse reflectance UV–vis spectra were recorded at ambient temperature on an EVOLUTION600 (ThermoScientific) spectrometer, using $BaSO_4$ as a reference. Spectra were recorded in the wavelength range of 200–600 nm. The bandgap was calculated from the following equation:

$$E = h \times C/\lambda$$

where h is Plank's constant (6.626×10^{-34} J/s), C is the speed of light (3.0×10^8 m/s), and λ is the cutoff wavelength (nanometers).

IR spectra in DRIFT mode of the different titania samples were recorded by using a Bruker Vertex spectrometer equipped with a liquid nitrogen-cooled MCT detector and a three-window DRIFTS (diffuse reflectance infrared Fourier transform spectroscopy) cell. In a typical experiment, 25 mg of the titania sample was heated to 393 K in He (30 mL/min) for 2 h, to remove the majority of adsorbed water. IR spectra were recorded before and after treatment. The spectrum of KBr was used as a background.

The photocatalytic activity was determined using an attenuated total reflectance–Fourier transform infrared (ATR–FTIR) setup.[16] The setup consists of a Harrick Horizon multiple-internal reflection accessory, equipped with a ZnSe crystal, and is enclosed by a top plate containing a quartz window, such that a 4 mL flow-through cell is obtained. The Fourier transform infrared measurements were again performed on the Bruker Vertex spectrometer equipped with the liquid nitrogen-cooled MCT detector. An assembly of seven LEDs (Roithner Lasertechnik) fitting on the top of the cell provided the illumination of the reaction mixture through the quartz window. Two different LED types were applied with two different wavelengths, 375 ± 10 and 425 ± 10 nm. The light intensity of the LEDs was fine-tuned to be equal at 1.5 mW/cm^2. The cell was completely isolated from stray light because it was covered with a nontransparent homemade box. Catalyst layers were prepared on the ATR crystal (ZnSe) as follows. A suspension of the photocatalyst (0.146 g/50 mL) in water was ultrasonicated for 30 min in a 35 kHz Elmasonic ultrasonic bath; 2 mL of this suspension was spread on the ZnSe crystal and dried in a vacuum overnight. MCH was saturated with O_2 by bubbling dry air at an 8 mL/min flow through the liquid for a few minutes. One milliliter of oxygen-saturated MCH was introduced to the catalyst layer on the ZnSe crystal. The cell was closed to prevent evaporation. Background spectra were recorded before illumination. The start of illumination was considered to be time zero of the reaction, after which spectra were recorded at fixed time intervals (typically 5 min) from 4000 to 700 cm^{-1} by collecting 64 scans with a resolution of 4 cm^{-1}.

RESULTS

The textural structure of the reduced titania sample was examined by nitrogen physisorption. The nitrogen adsorption–desorption isotherms and Barret–Joyner–Halenda (BJH) pore size distribution curves of the prepared sample and a commercial rutile sample are compared in Figure S1 (Supporting Information).

The reduced titania shows a type IV adsorption–desorption isotherm with an H2 hysteresis loop (which appears at 0.65 < P/P_o < 1), which is typical for mesoporous materials. Herein, the presence of mesopores is most likely the result of the aggregation of primary nanoparticles. The BET surface area derived from the isotherm is 22 m^2/g. The corresponding BJH pore size distribution of the sample is centered at 9 nm.

The XRD pattern of the blue titania is shown in Figure 1A. The pattern exhibits strong diffraction lines at 27°, 36°, and 55°

dx.doi.org/10.1021/cs300593d | ACS Catal. 2012, 2, 2641–2647

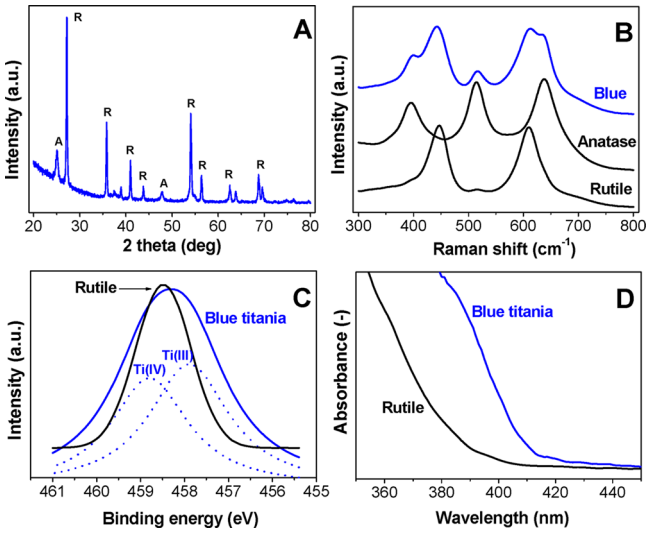

Figure 1. (A) XRD pattern of the blue titania sample. R refers to the characteristic peaks of the rutile phase, while A refers to anatase. (B) Raman spectrum of the blue titania sample compared with those of anatase and rutile samples. (C) XPS Ti2p 458.2 eV band of the blue titania as compared to that of rutile (solid line). The dotted lines are the deconvoluted signals of the blue titania band. (D) UV−vis spectrum of the blue titania as compared to that of the rutile sample.

indicating the presence of TiO_2 in the rutile phase. At the same time, the pattern exhibits strong diffraction lines at 25° and 48° indicating the presence of TiO_2 in the anatase phase. The anatase:rutile ratio in the reduced titania sample is estimated to be 15:85%.

The Raman spectrum of the reduced titana is presented in Figure 1B, compared to the spectra of rutile and anatase. The appearance of the bands at 391, 443, 511, 605, and 633 cm^{-1} confirms the presence of rutile and anatase phases in the reduced titania.

XPS analysis was conducted to investigate the surface state of titanium. The standard binding energy of $Ti2p_{3/2}$ in a reference rutile sample shows a narrow band located around 458.4 eV assigned to Ti^{4+} (Figure 1C). However, a broad intensity profile, centered at 458.2 eV, was observed for the blue titania sample. The broadness of the peak in the reduced titania sample indicates multiple oxidation states of the surface. After deconvolution, the signal at 457.7 eV can be attributed to the presence of Ti^{3+}.[17,18] The relative content of Ti^{3+} in the surface of reduced TiO_2 was obtained by comparing the XPS peak areas and thus roughly estimated to be 50%. Besides information about Ti^{3+} content, the XPS data also suggest that the amount of carbon remaining in the sample is relatively small, at least in (the vicinity of) the surface (see Table S2 and an extended XPS survey in the Supporting Information).

The UV−vis spectrum of reduced titania is compared to the spectrum of rutile in Figure 1D. The spectrum of the reduced titania shows a red shift compared to that of neat rutile. The calculated bandgap of the reduced titania is 2.93 eV, which is smaller than that of rutile (3.08 eV).[19] In view of the XPS data described above, we explain the shift by the presence of Ti^{3+}, rather than by carbon incorporated into the catalyst structure.

Photocatalytic activity was determined in MCH oxidation by ATR−FTIR spectroscopy, as follows. The spectrum of MCH and the spectra of the expected products are presented in the Supporting Information (Figure S3). In general, MCH exhibits bands around 2919, 2852, 1448, 1375, 1365, 1263, and 1247 cm^{-1}. The bands at high wavenumbers (i.e., 2919 and 2852 cm^{-1}) correspond to the symmetric and antisymmetric (C−H) stretching modes.

The bands at 1448, 1375, and 1375 cm^{-1} are assigned to C−H bending modes of the methyl group. The band appearing at 1263 cm^{-1} can be assigned to the stretching vibration of the C−C bond. Different reference experiments were conducted to prove the synergy between light and the catalyst to promote the reaction. No photolytic products were observed after illumination of MCH for 30 min at the two applied wavelengths. Furthermore, TiO_2 (blue and commercial) did not induce MCH oxidation in the absence of light. Finally, as reported by our group previously,[20] the synthetized catalyst might contain very small amounts of remaining carbon from the synthesis step and hence might contribute to spectral changes. Therefore, a reference experiment was conducted in which only the coated layer of the catalyst was subjected to light for 2 h and potential products were monitored by FTIR. Only minor changes in spectral intensity were observed, which is in agreement with the small amount of carbon on the surface, as detected by XPS (Table S2 of the Supporting Information). These observations indicate that the surface of the catalyst is relatively clean.

The spectrum of the MCH/catalyst composition after it had been exposed to illumination at 425 nm for 100 min is presented in the left panel of Figure 2. After illumination of

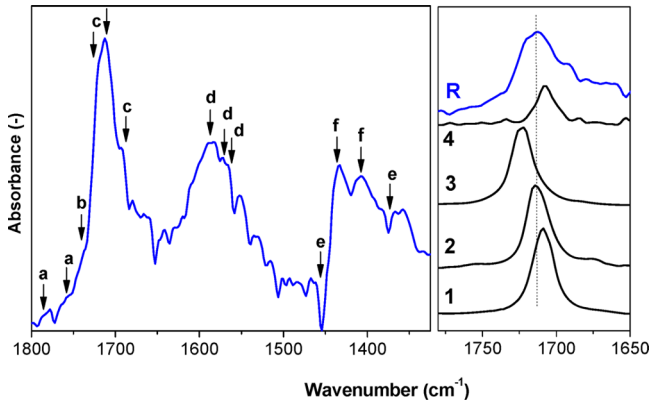

Figure 2. FTIR spectrum of MCH/catalyst (left) after illumination at 425 nm for 200 min: (a) formic acid, (b) formylcyclohexane, (c) methylcyclohexanone, adsorbed (1712 cm^{-1}) and dissolved (1685 cm^{-1}), (d) acetate or formate, (e) MCH, and (f) carbonate species. Spectrum of MCH (right) after reaction (R) as compared to reference spectra of **1**−**4**.

MCH interacting with the blue titania sample, a broad range of infrared absorptions develop in time between 1800 and 1000 cm^{-1}, an indication of the formation of several products. The photocatalytic oxidation of MCH can take place via two possible routes (Scheme 1). The first is the oxidation of the cyclic ring (I) with the formation of *o*- methylcyclohexanone (**1**) and/or *p*-methylcyclohexanone (**2**) as primary products. Overoxidation can take place, opening the ring and forming several carboxylate species as reported for cyclohexane.[16] The second oxidation route is the oxidation of the methyl group (II), with the formation of formylcyclohexane (**3**) as a primary product. Subsequent oxidation might form cyclohexanecarboxylic acid (**4**). The spectra of **1** and **2** show intensive bands at 1708 and 1714 cm^{-1}, respectively (Figure 2, right panel). The spectra of **3** and **4** exhibit dominant bands at 1724 and 1706

dx.doi.org/10.1021/cs300593d | ACS Catal. 2012, 2, 2641−2647

Scheme 1. Predicted Pathways of Photocatalytic Oxidation of MCH in the Liquid Phase

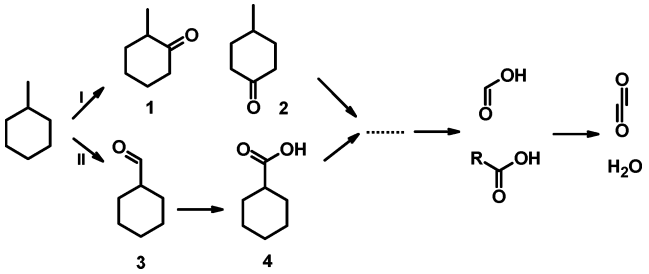

cm^{-1}, respectively. The bands at 1596, 1579, and 1564 cm^{-1} can be assigned to the ν_{as}(COO) mode of carboxylate species, and the band at 1403 cm^{-1} corresponds to the ν(C═O) mode of carbonate. Lastly, the bands at 1776, 1752, and 1569 cm^{-1} could be assigned to (formic) acid. The band assignments are summarized in Table S3 of the Supporting Information.

To identify the products of the photocatalytic oxidation of MCH, we compared the band locations in the range between 1650 and 1800 cm^{-1} with reference spectra (Figure 2, right panel). The comparison suggests the formation of **1** and **2** as major primary products, with a minor formation of **3**, which is totally absent in the beginning of the reaction (Figure S4 of the Supporting Information). **4** was difficult to identify because of the overlap with the band of **1**. However, because **4** is the overoxidation product of **3**, and **3** is minor, we propose route I as the main route for this reaction. This result does not agree with the observations of Alonso et al.,[21] who found **3** was the main product. This might be related to the different solvent (water) used by Alonso et al., as compared to neat methylcyclohexane in this study.

Furthermore, it is important to note that surface-adsorbed and -dissolved products (ketones) have absorptions at different wavenumbers. Mul et al.[16] reported a difference in the location of the band between dissolved cyclohexanone in cyclohexane (1712 cm^{-1}) and cyclohexanone adsorbed on the surface of Hombikat TiO_2 (1685 cm^{-1}) of ~25−30 wavenumbers, depending on the level of surface hydration.[22]

The IR spectra of MCH after reaction for 200 min over blue titania, photoexcited at 375 or 425 nm, are compared with those of rutile and P25 in Figure 3. It is clear that wavelength has a significant effect on the activity of the P25 sample, which is substantially smaller at 425 nm. The blue titania sample is photocatalytically more active than P25 and in particular than the rutile sample at both wavelengths, despite the higher surface area of the commercial samples (see Table S1 of the Supporting Information). Remarkably, the photocatalytic activity of blue TiO_2 is very similar at both wavelengths of illumination. Moreover, the product distribution seems to be almost the same, which is an indication that the reaction follows the same mechanism at the two different wavelengths. There is a significant difference in the product distribution between the blue titania sample and both the P25 and rutile catalysts (Figure 3). The ketone bands are more intense than the bands of carboxylates in the case of blue titania, while carboxylate contributions dominate in the spectra of P25 and rutile. Not only the activity but also the selectivity for the ketones seems to be lower at 425 nm for the rutile and P25 catalysts, although these are hard to determine as a result of the low level of conversion for the rutile catalyst and negative spectral contribution of adsorbed water for P25, respectively. An

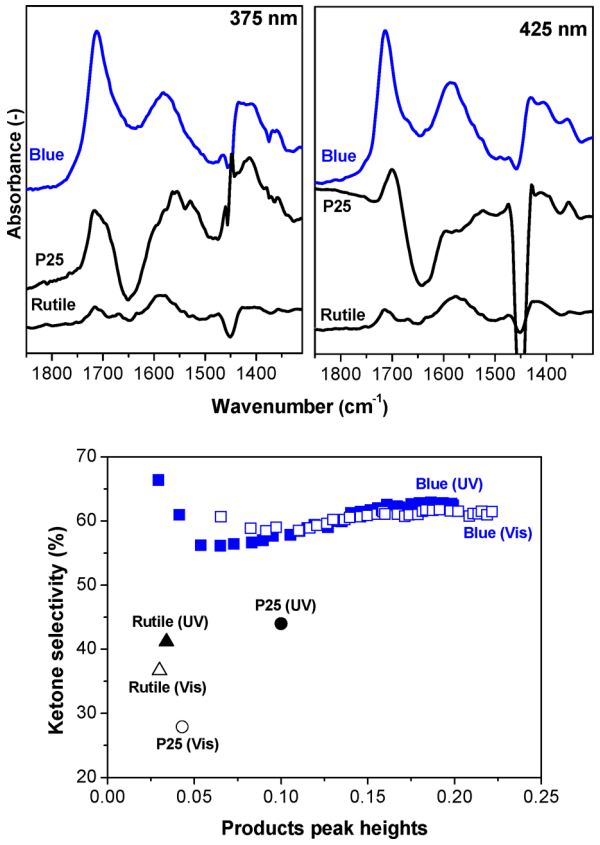

Figure 3. Collected spectra of MCH photo-oxidation (top) catalyzed by blue titania, P25, and rutile by excitation at 375 nm (left) or 425 nm (right). Ketone selectivity (bottom) plotted vs peak height (a measure of conversion) of the products.

indication of the quantity of ketones produced after reaction for 100 min under the two applied wavelengths is presented in Table 1. The amounts were determined on the basis of

Table 1. Amounts of Ketone (methylcyclohexanone) Produced after Illumination for 100 min

	amount of ketone (μmol)	
sample	375 nm	425 nm
blue titania	6.2	5.9
P25	2.7	2.1
rutile	0.8	0.7

calibration of the band intensity in the range of 1650−1750 cm^{-1}, as a function of concentration. The amounts allow calculation of a rate of approximately 3.8 μmol/h for blue titania at 375 nm, and a conversion of MCH (1 mL amounts to 8 mmol) to the ketones of approximately 0.05% after reaction for 1 h. Furthermore, given the used light intensity, a photonic efficiency to the ketones, defined as the number of moles produced per hour, divided by the number of photons entering the reactor per hour (8.5×10^{-5} einsteins/h for 375 nm and 9.7×10^{-5} einsteins/h for 425 nm) of 5% can be calculated, which is an order of magnitude lower for the rutile sample (0.6%). These are values on the same order of magnitude as typically observed in selective photocatalytic transformations using catalyst coatings, obviously largely influenced by the rate of deactivation of the various catalysts and applied reactor configuration.[23]

dx.doi.org/10.1021/cs300593d | ACS Catal. 2012, 2, 2641−2647

Additional information about the ketone selectivity for blue TiO_2 was obtained by analyzing the time-dependent evolution of the height of the ketone band at 1716 cm^{-1} relative to that of the carboxylate band at 1579 cm^{-1}. The development of these two bands is demonstrated in Figure S4 of the Supporting Information. Figure S4 proves the high degree of similarity of product formation upon excitation at 375 and 425 nm. The amounts of products formed on the surface of blue titania seem to increase by the same rate, the product distribution at the different applied wavelengths (UV and visible illumination) also being very similar. The selectivity for ketones initially slightly decreases to a rather constant value of 55−60% at extended reaction times (see also Figure 3), under either UV or visible light illumination. A lower selectivity for ketones was obtained in the case of either rutile or P25 after reaction for 200 min. Furthermore, the ratio between the adsorbed and dissolved ketones seems higher in the case of P25 than in the case of the blue titania sample, via analysis of the bands in the ketone range in detail. This might have implications for the obtained selectivity, to be discussed in the next paragraph.

DISCUSSION

Generally, three main differences were found in the properties of the catalysts used in this study (i.e., blue TiO_2, P25, and rutile TiO_2): (1) the textural properties, (2) the phase composition, and (3) the presence or absence of (surface) defects. These three aspects are relevant for explaining the differences in photocatalytic activity and product selectivity in the photo-oxidation of MCH.

First, a correlation between the surface area and the photocatalytic activity of the three titania catalysts was not found: the surface areas of P25 and rutile are significantly higher than that of the blue titania (see Table S1 of the Supporting Information), whereas the latter shows the highest activity.

The phase composition of the three samples is an interesting issue to discuss. TiO_2 in the rutile form has often been demonstrated to be less photoactive than TiO_2 in the anatase form.[24] This is in agreement with the results obtained here, where rutile hardly activates the photo-oxidation of MCH when exposed to the two applied wavelengths, even though rutile has a smaller bandgap (3.05 eV) than anatase (3.2 eV) and hence shows a small red shift in the absorption spectrum. The coexistence of rutile and anatase in P25 (23% rutile and 77% anatase) has often been reported to be responsible for the enhanced activity of this catalyst as compared to those of anatase and rutile, explained by more effective charge separation (i.e., the antenna theory).[25] The relationship between the phase composition and the photocatalytic activity of TiO_2 was also recently discussed by Li et al.[26] In the evolution of H_2 from methanol/water solutions, these authors found important synergy between anatase and rutile if relatively small crystals of anatase were dispersed on larger rutile crystals, attributed to the formation of a surface anatase−rutile phase junction. To determine if the phase composition of the Ti^{3+}-containing blue TiO_2 is a dominant factor in determining the activity, an experiment was performed in which we prepared a physical mixture of commercial rutile and anatase with the same ratio as in the blue titania sample (i.e., 15% anatase and 85% anatase). A negligible synergy was found under UV illumination, which is in good agreement with the studies of Mul[27] and Besenbacher.[28] While we realize that the interaction in a physical mixture does not fully represent the nature of the interaction between the two phases in the blue titania sample, we feel the coexistence of rutile and anatase phases is not the main reason for the higher photocatalytic activity in MCH oxidation of the neat Ti^{3+}-containing catalyst.

A high photocatalytic activity of reduced TiO_2 under visible light illumination was observed previously. Mao et al.[6] recently reported a high photocatalytic activity of a black titania (hydrogenated titania) in the water splitting reaction, as well as in methylene blue degradation. Feng et al.[7] also reported a blue, reduced titania form, doped with Pt as an active catalyst for water splitting. Hashimoto et al.[29] reported Cu-modified titania as an active catalyst for the photon-induced decomposition of 2-propanol. The reason for the high visible light-induced activity of the reduced titania was explained by the generation of sublevels in the bandgap as a result of the presence of Ti^{3+}, with an energy somewhat lower than the conduction band minimum of stoichiometric (Ti^{4+}) TiO_2.[6,29] Under UV illumination, a TiO_2 photocatalyst will absorb light of sufficient energy, upon which an electron−hole pair is formed (eq 1), representing the photon-excited state. The energy of the photon-excited electron is dependent on the conduction band energy level or the generated sublevel. The electron will react with O_2 to form a super oxide anion, which will contribute to oxidation of MCH to form **1**, **2**, or **3** and most likely cause the (re)oxidation of the TiO_2 surface.[30] Consecutive oxidation processes will open the ring to form carboxylate compounds. The holes will react with surface OH groups or with water to form strongly oxidizing OH radicals. The hydroxyl radicals are necessary for the primary and secondary activation of the hydrocarbon but also, most likely, will contribute to the degradation of MCH to carboxylates, and eventually to CO_2 and H_2O.

Under visible light illumination, globally the same elementary steps will occur for blue TiO_2, with the exception that now the majority of the catalytically active excited state electrons will reside on the surface defect (Ti^{3+}) sites. However, these electrons, and the similar energetic state of the holes, will lead to the same redox reactions and thus to the same catalytic selectivity. The absence of a significant enhancement in rate with an increase in the energy of the photons to 375 nm suggests that the Ti^{3+} centers are also dominating catalysis at this higher energetic radiation, possibly because these are the sites favoring O_2 adsorption. The excess energy of the 375 nm radiation is apparently lost by recombination of conduction band electrons and holes, or by relaxation of the conduction band electron to the state of the defect site, either radiatively or nonradiatively.

The arguments given above suggest that the presence of the defect V_O-Ti^{3+} sites induces the high activity either upon UV illumination or upon visible light illumination. Another separate experiment was conducted to confirm this concept: a new batch of blue titania was prepared with only three-quarters of the amount of the reducing agents (i.e., ethanol and ethylimidazole). The aim was to produce less reducing gases and to create fewer defect sites. After reaction for 200 min under illumination at 375 nm, it was clear that the photocatalytic activity of this catalyst is significantly smaller than of the catalyst containing a higher concentration of V_O-Ti^{3+} sites. A remaining issue concerns the location of the surface defect sites, whether these are predominantly present at the rutile or anatase surface. Given the high rutile content of our sample and the excellent performance of reduced rutile in water decomposition as reported in the literature,[6] intuitively we favor the hypothesis

dx.doi.org/10.1021/cs300593d | ACS Catal. 2012, 2, 2641−2647

that these are located on the rutile phase. The presence and function of reduced anatase sites in our composition require further investigation.

The difference in ketone selectivity between the various catalysts can most likely be explained by the nature of the catalyst surface and its affinity for water. Surface-adsorbed water stimulates desorption of product, beneficial for selectivity, but also promotes the generation of hydroxyl radicals, which likely leads to higher rates of overoxidation and thus carboxylate production. To study the affinity of the blue titania for water compared to that of the commercial titania catalysts, the surface of each catalyst was kept at 393 K in a helium environment for 2 h, followed by collection of IR spectra in DRIFT mode. The spectra showed a much greater affinity of P25 for water compared to that of blue titania (Figure 4, left panel), in

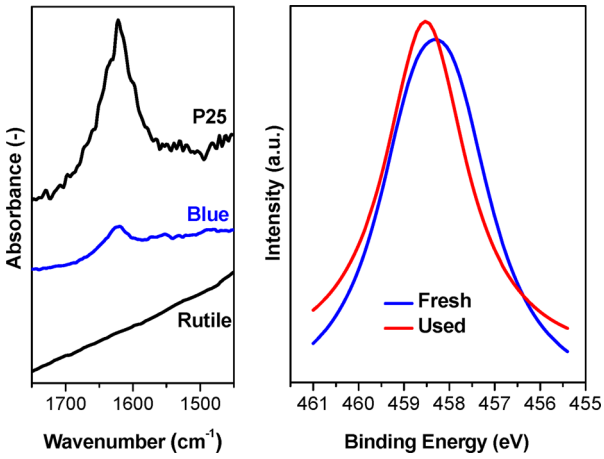

Figure 4. IR spectra of blue titania (left) compared to those of P25 and rutile. XPS Ti2p 458.1 eV band of the blue titania sample (right) before the reaction (Fresh) and after the reaction (Used).

agreement with the differences in selectivity. Another indication of the higher level of surface hydration follows from the collected ATR–FTIR spectra of the MCH after the reaction. A higher ratio of desorbed ketone species to adsorbed species is apparent in the case of P25 compared to the case of the blue titania sample (Figure 3), in agreement with the higher state of hydration of the P25 catalyst.[31] The rutile catalyst shows an extremely low affinity for water. The low selectivity of the rutile catalyst thus appears to be related to an intense interaction between the product and the surface. This requires further investigation.

Although the blue titania catalyst showed better photoactivity and higher ketone selectivity than the commercial titania catalysts, this catalyst could not maintain such activity for long periods of time (Figure S5 of the Supporting Information) and was largely deactivated after the first run. The high photoactivity of the blue titania was attributed to the presence of Ti^{3+} (above); thus, besides the commonly observed detrimental effects of the adsorbed carboxylates and carbonates, a reduction in the amount of Ti^{3+} might contribute to catalyst deactivation. The XPS spectrum for the used blue titania was recorded after the reaction and compared with that of the fresh blue tiania sample (Figure 4, right panel). It is obvious that the area representing the reduced Ti^{3+} sites was smaller after reaction. This is an indication that the concentration of Ti^{3+} decreases during the reaction. The reason for the deactivation might be explained by the reaction proposed previously by Takeuchi et al.[32] and also by Harima et al.[33] in which Ti^{3+} in the presence of oxygen may undergo oxidation to Ti^{4+} as follows:

$$Ti^{3+} - Ti^{3+} + O_2 \rightarrow Ti^{4+} - O_2^{2-} - Ti^{4+} \quad (1)$$

To conclude, the prepared sample is a mesoporous titania with bluish gray color. The surface area of the sample is 22 cm^2/g, and the average pore diameter is 9 nm. The sample consists of 85% rutile and 15% anatase with the presence of surface Ti^{3+} in an estimated amount of 50% of all surface sites. The sample showed a red-shifted UV–vis absorption, with a calculated bandgap at 2.93 eV. The blue titania is a more active photocatalyst than either P25 or commercial rutile titania, when applied in the oxidation of MCH, in particular at 425 nm. Blue titania also shows higher selectivity for the production of ketones. These phenomena are mostly related to a high concentration of surface defect sites (Ti^{3+}) and a relatively low but still significant affinity for water. The catalyst unfortunately showed deactivation as a result of photoinduced oxidation of Ti^{3+} to Ti^{4+} by molecular oxygen. The promotion of electron and oxygen transfer reactions by including (noble) metal particles with the reduced catalyst is currently under investigation, to determine if this is beneficial for catalyst stability and performance in general.

■ ASSOCIATED CONTENT

Supporting Information

Textural properties of blue titania compared with those of rutile and P25, collected spectra of MCH oxidation after reaction for 200 min, and peak identification. This material is available free of charge via the Internet at http://pubs.acs.org.

■ AUTHOR INFORMATION

Corresponding Author

*Photocatalytic Synthesis Group, Faculty of Science and Technology, MESA+ Institute for Nanotechnology, University of Twente, P.O. Box 217, 7500 AE Enschede, The Netherlands. Fax: (+)31 53 4892882. Telephone: (+)31 53 4893890. E-mail: g.mul@utwente.nl.

Notes

The authors declare no competing financial interest.

■ ACKNOWLEDGMENTS

We thank Mr. Robert Meijer for the excellent technical assistance, Mr. Gerard Kip for performing the XPS measurements, and Mrs. Louise Vrielink for N_2 physisorption measurements.

■ REFERENCES

(1) Klosek, S.; Raftery, D. *J. Phys. Chem. B* **2001**, *105*, 2815.
(2) Zhang, S.; Chen, Y.; Yu, Y.; Wu, H.; Wang, S.; Zhu, B.; Huang, W.; Wu, S. *J. Nanopart. Res.* **2008**, *10*, 871.
(3) Yu, S.; Yun, H. J.; Lee, D. M.; Yi, J. *J. Mater. Chem.* **2012**, *22*, 12629.
(4) Cong, Y.; Zhang, J.; Chen, F.; Anpo, M. *J. Phys. Chem. C* **2007**, *111*, 6976.
(5) Chen, F.; Zou, W.; Qu, W.; Zhang, J. *Catal. Commun.* **2009**, *10*, 1510.
(6) Chen, X.; Liu, L.; Yu, P. Y.; Mao, S. S. *Science* **2011**, *331*, 746.
(7) Zuo, F.; Wang, L.; Wu, T.; Zhang, Z.; Borchardt, D.; Feng, P. *J. Am. Chem. Soc.* **2010**, *132*, 11856.
(8) Liu, H.; Ma, H. T.; Li, X. Z.; Li, W. Z.; Wu, M.; Bao, X. H. *Chemosphere* **2003**, *50*, 39.

(9) Sirisuk, A.; Klansorn, E.; Praserthdam, P. *Catal. Commun.* **2008**, *9*, 1810.
(10) Henrich, V. E.; Kurtz, R. L. *Phys. Rev. B* **1981**, *23*, 6280.
(11) Lu, G.; Linsebigler, A.; Yates, J. T. *J. Phys. Chem.* **1994**, *98*, 11733.
(12) Li, Y.; Li, X.; Li, J.; Yin, J. *Mater. Lett.* **2005**, *59*, 2659.
(13) Le Mercier, T.; Mariot, J. M.; Parent, P.; Fontaine, M. F.; Hague, C. F.; Quarton, M. *Appl. Surf. Sci.* **1995**, *86*, 382.
(14) Lu, T.-C.; Lin, L.-B.; Wu, S.-Y.; Zhao, C.-P.; Xu, X.-C.; Tian, Y.-F. *Nucl. Instrum. Methods Phys. Res., Sect. B* **2002**, *191*, 291.
(15) Dohshi, S.; Anpo, M.; Okuda, S.; Kojima, T. *Top. Catal.* **2005**, *35*, 327.
(16) Almeida, A. R.; Moulijn, J. A.; Mul, G. *J. Phys. Chem. C* **2008**, *112*, 1552.
(17) Pan, J.; Wu, X.; Wang, L.; Liu, G.; Lub, G. Q.; Cheng, H.-M. *Chem. Commun.* **2011**, *47*, 8361.
(18) Lee, Y. C.; Hong, Y. P.; Lee, H. Y.; Kim, H.; Jung, Y. J.; Ko, K. H.; Jung, H. S.; Hong, K. S. *J. Colloid Interface Sci.* **2003**, *267*, 127.
(19) Livraghi, S.; Maurelli, S.; Paganini, M. C.; Chiesa, M.; Giamello, E. *Angew. Chem., Int. Ed.* **2011**, *50*, 8038.
(20) Yang, C.-C.; Yu, Y.-H.; van der Linden, B.; Wu, J. C. S.; Mul, G. *J. Am. Chem. Soc.* **2010**, *132*, 8398.
(21) Hernández-Alonso, M. D.; Tejedor-Tejedor, I.; Coronado, J. M.; Anderson, M. A. *Appl. Catal., B* **2011**, *101*, 283.
(22) Almeida, A. R.; Calatayud, M.; Tielens, F.; Moulijn, J. A.; Mul, G. *J. Phys. Chem. C* **2011**, *115*, 14164.
(23) Du, P.; Carneiro, J. T.; Moulijn, J. A.; Mul, G. *Appl. Catal., A* **2008**, *334*, 119.
(24) Addamo, M.; Bellardita, M.; Di Paola, A.; Palmisano, L. *Chem. Commun.* **2006**, 4943.
(25) Hurum, D. C.; Agrios, A. G.; Gray, K. A.; Rajh, T.; Thurnauer, M. C. *J. Phys. Chem. B* **2003**, *107*, 4545.
(26) Zhang, J.; Xu, Q.; Feng, Z.; Li, M.; Li, C. *Angew. Chem.* **2008**, *120*, 1790.
(27) Carneiro, J. T.; Savenije, T. J.; Moulijn, J. A.; Mul, G. *J. Phys. Chem. C* **2011**, *115*, 2211.
(28) Su, R.; Bechstein, R.; Sø, L.; Vang, R. T.; Sillassen, M.; Esbjörnsson, B.; Palmqvist, A.; Besenbacher, F. *J. Phys. Chem. C* **2011**, *115*, 24287.
(29) Liu, M.; Qiu, X.; Miyauchi, M.; Hashimoto, K. *Chem. Mater.* **2011**, *23*, 5282.
(30) Almeida, A. R.; Moulijn, J. A.; Mul, G. *J. Phys. Chem. C* **2011**, *115*, 1330.
(31) Renckens, T. J. A.; Almeida, A. R.; Damen, M. R.; Kreutzer, M. T.; Mul, G. *Catal. Today* **2010**, *155*, 302.
(32) Takeuchi, M.; Martra, G.; Coluccia, S.; Anpo, M. *J. Phys. Chem. C* **2007**, *111*, 9811.
(33) Komaguchi, K.; Maruoka, T.; Nakano, H.; Imae, I.; Ooyama, Y.; Harima, Y. *J. Phys. Chem. C* **2009**, *114*, 1240.